

Modeling and reliability analysis of three phase z-source AC-AC converter

HANUMAN PRASAD¹, TANMOY MAITY²

¹*Department of Electrical Engineering
Sandip Institute of Engineering and Management
Nashik, India*

²*Department of Mining Machinery Engineering
Indian Institute of Technology (Indian School of Mines)
Dhanbad, India
e-mail: hpshukla271@gmail.com*

(Received: 24.04.2017, revised: 21.07.2017)

Abstract: This paper presents the small signal modeling using the state space averaging technique and reliability analysis of a three-phase z-source ac-ac converter. By controlling the shoot-through duty ratio, it can operate in buck-boost mode and maintain desired output voltage during voltage sag and surge condition. It has faster dynamic response and higher efficiency as compared to the traditional voltage regulator. Small signal analysis derives different control transfer functions and this leads to design a suitable controller for a closed loop system during supply voltage variation. The closed loop system of the converter with a PID controller eliminates the transients in output voltage and provides steady state regulated output. The proposed model designed in the RT-LAB and executed in a field programming gate array (FPGA)-based real-time digital simulator at a fixed-time step of 10 μ s and a constant switching frequency of 10 kHz. The simulator was developed using very high speed integrated circuit hardware description language (VHDL), making it versatile and moveable. Hardware-in-the-loop (HIL) simulation results are presented to justify the MATLAB simulation results during supply voltage variation of the three phase z-source ac-ac converter. The reliability analysis has been applied to the converter to find out the failure rate of its different components.

Key words: real-time digital simulation (RTDS), field programming gate array (FPGA), hardware-in-the-loop (HIL), z-source ac-ac converter, PID controller

1. Introduction

Real-time simulators are innovative apparatus to demonstrate in many engineering fields such as power system, aircraft design, industrial automation, power grid protection tests and power electronics based motor drives applications for design, development and testing of the prototype system [1-2]. The FPGA-based real-time simulators computed the proposed design model with calculated time-step i.e. equivalent to the real-world clock. The offline simulation

software such as EMTP, PSIM, MATLAB/Simulink and PSCAD executed the model with a variable step solver and execution time depends on different parameters such as complexity of the system, RAM, processor speed and an operating system etc. It cannot interface the actual hardware while this is possible in a real-time simulator. RT-LAB is fully incorporated with MATLAB/Simulink and generated the hardware description languages (HDL) code automatically without any hand written code in Xilinx System Generator (XSG). The FPGA-based real-time simulator has been developed as a primary movement for HIL applications, which executed the proposed model in real-time embedded control with designated time value for power electronics applications [3-5]. It provides a reliable, effective and non-destructive method in the design, development, and testing of the prototype system. In this technique, a virtual plant executed in the simulator and a hardware prototype controller plant interface with the simulator. The host computer and target (RTDS) are communicated with an Ethernet cable. The proposed real-time HIL test approach is applied in a three phase z-source ac-ac converter during voltage sag and surge condition.

A z-source converter especially as an inverter [6] is a popular topology nowadays. It consists of an impedance network between a DC power source and the main converter bridge circuit. The z-source inverter removes the constraint of the traditional voltage source and current source inverter. By controlling the shoot-through duty ratio, it can operate in buck-boost mode. In the case of ac-ac conversion, the z-source topology is proposed for a single phase application [7-8]. Three phase z-source ac-ac converters are also proposed [9-11] employing three inductors, three capacitors, six bi-directional switches etc. This is a single stage buck-boost switching voltage regulator which enhances system efficiency and reduces cost of the system. The impedance network stores or releases energy accordingly to drive the circuit as a perfect regulator. A traditional three phase ac-ac voltage regulator is operated at lower efficiency as compared to a z-source ac-ac converter. By controlling the shoot-through duty ratio, a single phase z-source ac-ac converter can produce regulated output voltage during voltage sag and surge [12].

A small signal models of a PWM converter are normally followed by state space averaging [13] and circuit averaging [14] techniques. The state space averaging technique may be applied to the three phase z-source converter associated with the averaging of the state equations during shoot-through and non-shoot-through switching states. Circuit averaging is achieved by the switching component waveform. The state space averaging technique approach has a number of advantages over the circuit averaging technique like compact representation of equations, ability to obtain more transfer functions etc. The small signal analysis of the converter adds steady state values with consideration of mathematical perturbation. The small signal and signal-flow-graph modeling of a switched z-source inverter impedance network is discussed in [15]. The stability analysis of a control transfer function indicates the system's stability. The non-minimum phase transfer function increases system robustness. The RHP zero may not be shifted to the left side by adjusting z-network parameters but it increases system losses and the settling time. The transient modeling and analysis of a PWM z-source inverter is discussed in [16-17] which focuses on the transient analysis of the dc and ac side of the converter. The dc analysis is based on small signal and signal flow graph of the impedance network and the ac

side analysis gives space analysis representation of the inverter output voltage. Again, three phase circuit modeling through abc to dq transformation eliminates time varying nature of transformation that gives accurate and reliable modeling of a converter [18-19]. It derives more efficient and effective control transfer functions. The paper [20] discussed the steady state analysis and derived the transfer function for both ideal and non-ideal PWM z-source DC-DC converters.

Power Electronics semiconductor devices are more complicated to design as a system component. The probability of the system is the operating time period of the system components. The reliability analysis of parallel components is defined as one component operates through the whole time period from beginning to ending, such type of system is called perfect reliable. The paper [21] focuses on the general reliability of the parallel components in the form of reliability function and literature [22] discussed the reliability analysis and optimization of the integrated circuit. The integrated devices reduce the leakage current of semiconductor switching devices for a long time period. A large scale technology increases the complexity and losses in the system. The reliability of an individual component is discussed in a military hand book and few publications [23-24]. More reliability is required for specific application such as military aircraft, space etc. The reliability concerns the failure of component, mechanism and effect analysis of different components under different operating condition. The converter operating under a closed loop condition is affected by any variation in one component; the other components are also affected by this variation. In the proposed work, calculation of time varied reliability of the converter with respect of system component of the circuit is performed. Reliability of individual component and its mean time-to failure are derived for the three phase z-source ac-ac converter.

The circuit topology of the three phase z-source ac-ac converter is shown in Fig. 1. There are two switching states in this converter circuit. In the non-shoot through state the bi-directional switches S1, S2, S3 are turned on all together and S4, S5, S6 are turned off all together and the corresponding equivalent circuit is shown in Fig. 2. The ac source charges the z-network capacitors as well as energy is transferred to the load by the inductor. The operating interval of the converter in this state is $(1 - D)T$, where D is the duty ratio of switch S4, S5, S6 and T is the switching cycle. During the shoot-through state the bi-directional switches S1, S2 and S3 are turned off and S4, S5, and S6 are turned on and the operating time interval is DT as shown in Fig. 3.

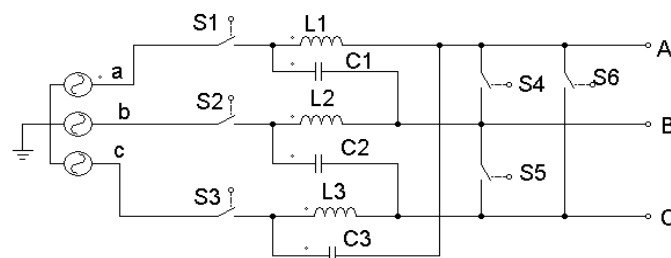


Fig. 1. Equivalent circuit of the three phase ac-ac circuit

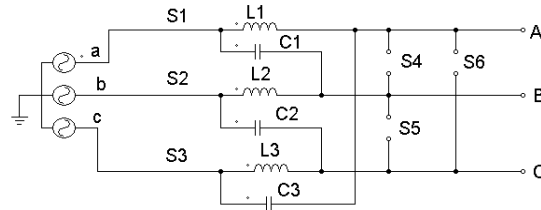


Fig. 2. Non-shoot through state of the three phase ac-ac circuit

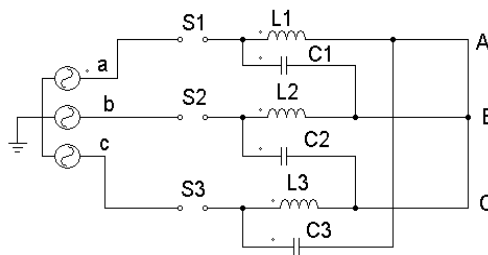


Fig. 3. Shoot-through equivalent circuit of the three phase ac-ac circuit

Here the electrostatic energy of the capacitor is stored in the inductor which is utilized to boost the output voltage during the non-shoot through state. The topology helps to operate the converter in the boost mode when D is below 0.5 and in the buck mode when D is set above 0.5. The maximum gain of the converter achievable is 1.15.

2. Small signal modeling

Small signal analysis is a linearization of the nonlinear devices. Some assumptions have been taken for small signal analysis. These are:

- 1) A converter is operating in continuous conduction mode.
- 2) All semiconductor devices i.e. IGBT and a diode are operated as an ideal switch and lossless.
- 3) The passive component such as a resistor, inductor and capacitor are linear, time invariant and frequency independent.
- 4) Natural time constant of the converter is more than one switching time period.

Small signal analysis by a state space averaging technique is used to present the state equation of switching states. The three phase z-source ac-ac converter has six energy storage elements i.e. three capacitors and three inductors. Hence the three phase z-source converter system has six state variables.

Now, assuming input line voltages as V_{ab} , V_{bc} , V_{ca} output voltages as V_{o1} , V_{o2} , V_{o3} current through inductors L_1 , L_2 and L_3 as I_{L1} , I_{L2} and I_{L3} respectively, voltage across capacitors C_1 , C_2 and C_3 as V_{C1} , V_{C2} and V_{C3} respectively, output current per phase as I_{o1} , I_{o2} and I_{o3} and input current per phase as i_a , i_b and i_c .

Also, considering the order of the system = 6, states of the system

$$x = \begin{bmatrix} i_{L_1} \\ i_{L_2} \\ i_{L_3} \\ V_{C_1} \\ V_{C_2} \\ V_{C_3} \end{bmatrix}, \text{ input of the system } u = \begin{bmatrix} V_{ab} \\ V_{bc} \\ V_{ca} \\ I_{o1} \\ I_{o2} \\ I_{o3} \end{bmatrix}, \text{ output of the system } y = \begin{bmatrix} V_{o1} \\ V_{o2} \\ V_{o3} \\ i_a \\ i_b \\ i_c \end{bmatrix}$$

The state equation during the non-shoot through state referring to Fig. 2 becomes:

$$\begin{bmatrix} \dot{i}_{L_1} \\ \dot{i}_{L_2} \\ \dot{i}_{L_3} \\ \dot{V}_{C_1} \\ \dot{V}_{C_2} \\ \dot{V}_{C_3} \end{bmatrix} = \begin{bmatrix} 0 & 0 & 0 & 0 & 0 & \frac{1}{L_1} \\ 0 & 0 & 0 & \frac{1}{L_2} & 0 & 0 \\ 0 & 0 & 0 & 0 & \frac{1}{L_3} & 0 \\ 0 & -\frac{1}{C_1} & 0 & 0 & 0 & 0 \\ 0 & 0 & -\frac{1}{C_2} & 0 & 0 & 0 \\ -\frac{1}{C_3} & 0 & 0 & 0 & 0 & 0 \end{bmatrix} \begin{bmatrix} i_{L_1} \\ i_{L_2} \\ i_{L_3} \\ V_{C_1} \\ V_{C_2} \\ V_{C_3} \end{bmatrix} + \begin{bmatrix} 0 & 0 & -\frac{1}{L_1} & 0 & 0 & 0 \\ -\frac{1}{L_2} & 0 & 0 & 0 & 0 & 0 \\ 0 & -\frac{1}{L_3} & 0 & 0 & 0 & 0 \\ 0 & 0 & 0 & 0 & \frac{1}{C_1} & 0 \\ 0 & 0 & 0 & 0 & 0 & \frac{1}{C_2} \\ 0 & 0 & 0 & \frac{1}{C_3} & 0 & 0 \end{bmatrix} \begin{bmatrix} V_{ab} \\ V_{bc} \\ V_{ca} \\ i_{o1} \\ i_{o2} \\ i_{o3} \end{bmatrix} \quad (1)$$

Similarly for the shoot through state, the Fig. 3 gives the state equation

$$\begin{bmatrix} \dot{i}_{L_1} \\ \dot{i}_{L_2} \\ \dot{i}_{L_3} \\ \dot{V}_{C_1} \\ \dot{V}_{C_2} \\ \dot{V}_{C_3} \end{bmatrix} = \begin{bmatrix} 0 & 0 & 0 & \frac{1}{L_1} & 0 & 0 \\ 0 & 0 & 0 & 0 & \frac{1}{L_2} & 0 \\ 0 & 0 & 0 & 0 & 0 & \frac{1}{L_3} \\ -\frac{1}{C_1} & 0 & 0 & 0 & 0 & 0 \\ 0 & -\frac{1}{C_2} & 0 & 0 & 0 & 0 \\ 0 & 0 & -\frac{1}{C_3} & 0 & 0 & 0 \end{bmatrix} \begin{bmatrix} i_{L_1} \\ i_{L_2} \\ i_{L_3} \\ V_{C_1} \\ V_{C_2} \\ V_{C_3} \end{bmatrix} + [0] \begin{bmatrix} V_{ab} \\ V_{bc} \\ V_{ca} \\ i_{o1} \\ i_{o2} \\ i_{o3} \end{bmatrix} \quad (2)$$

Equations (1) and (2) are converted into the d - q co-ordinate system for proper analysis. Equal values of inductance and capacitance are chosen for the circuit simplicity like $L_1 = L_2 = L_3 = L$, $C_1 = C_2 = C_3 = C$, and was supply frequency.

After the d - q transformation, the state equation during the non-shoot through state becomes:

$$\begin{bmatrix} \dot{i}_{Ld} \\ \dot{i}_{Lq} \\ \dot{i}_{Lo} \\ \dot{V}_{Cd} \\ \dot{V}_{Cq} \\ \dot{V}_{Co} \end{bmatrix} = \begin{bmatrix} 0 & w & 0 & -\frac{1}{2L} & -\frac{\sqrt{3}}{2L} & 0 \\ -w & 0 & 0 & \frac{\sqrt{3}}{2L} & -\frac{1}{2L} & 0 \\ 0 & 0 & 0 & 0 & 0 & \frac{1}{L} \\ \frac{1}{2C} & -\frac{\sqrt{3}}{2C} & 0 & 0 & w & 0 \\ \frac{\sqrt{3}}{2C} & \frac{1}{2C} & 0 & -w & 0 & 0 \\ 0 & 0 & -\frac{1}{C} & 0 & 0 & 0 \end{bmatrix} \begin{bmatrix} i_{Ld} \\ i_{Lq} \\ i_{Lo} \\ V_{Cd} \\ V_{Cq} \\ V_{Co} \end{bmatrix} + \begin{bmatrix} \frac{1}{2L} & \frac{\sqrt{3}}{2L} & 0 & 0 & 0 & 0 \\ -\frac{\sqrt{3}}{2L} & \frac{1}{2L} & 0 & 0 & 0 & 0 \\ 0 & 0 & -\frac{1}{L} & 0 & 0 & 0 \\ 0 & 0 & 0 & -\frac{1}{2C} & \frac{\sqrt{3}}{2C} & 0 \\ 0 & 0 & 0 & \frac{\sqrt{3}}{2C} & -\frac{1}{2C} & 0 \\ 0 & 0 & 0 & 0 & 0 & \frac{1}{C} \end{bmatrix} \begin{bmatrix} V_{id} \\ V_{iq} \\ V_{io} \\ i_{od} \\ i_{oq} \\ i_{oo} \end{bmatrix} \quad (3)$$

Similarly, after the d - q transformation, state equation in the shoot through state becomes:

$$\begin{bmatrix} \dot{i}_{Ld} \\ \dot{i}_{Lq} \\ \dot{i}_{Lo} \\ \dot{V}_{Cd} \\ \dot{V}_{Cq} \\ \dot{V}_{Co} \end{bmatrix} = \begin{bmatrix} 0 & w & 0 & \frac{1}{L} & 0 & 0 \\ -w & 0 & 0 & 0 & \frac{1}{L} & 0 \\ 0 & 0 & 0 & 0 & 0 & \frac{1}{L} \\ -\frac{1}{C} & 0 & 0 & 0 & w & 0 \\ 0 & -\frac{1}{C} & 0 & -w & 0 & 0 \\ 0 & 0 & -\frac{1}{C} & 0 & 0 & 0 \end{bmatrix} \begin{bmatrix} i_{Ld} \\ i_{Lq} \\ i_{Lo} \\ V_{Cd} \\ V_{Cq} \\ V_{Co} \end{bmatrix} + [0] \begin{bmatrix} V_{id} \\ V_{iq} \\ V_{io} \\ i_{od} \\ i_{oq} \\ i_{oo} \end{bmatrix} \quad (4)$$

Applying perturbation in the signals like:

$$v_{abc} = V_{abc} + \widehat{V}_{abc},$$

$$i_{abc} = I_{abc} + \widehat{i}_{abc},$$

$$i_{L_1L_2L_3} = I_{L_1L_2L_3} + \widehat{i}_{L_1L_2L_3},$$

$$v_{C_1C_2C_3} = V_{C_1C_2C_3} + \widehat{V}_{C_1C_2C_3},$$

$$v_{o1o2o3} = V_{o1o2o3} + \widehat{V}_{o1o2o3},$$

$$i_{o1o2o3} = I_{o1o2o3} + \widehat{i}_{o1o2o3},$$

$$d = D + \widehat{d},$$

where V_{abc} , I_{abc} , $I_{L_1L_2L_3}$, $V_{C_1C_2C_3}$, V_{o1o2o3} , I_{o1o2o3} , D are the steady state values and \widehat{V}_{abc} , \widehat{i}_{abc} , $\widehat{i}_{L_1L_2L_3}$, $\widehat{V}_{C_1C_2C_3}$, \widehat{V}_{o1o2o3} , \widehat{i}_{o1o2o3} , \widehat{d} are corresponding small signal values.

Hence, we obtain the state space averaging equation as (5).

$$\begin{bmatrix} \dot{i}_{Ld} \\ \dot{i}_{Lq} \\ \dot{i}_{Lo} \\ \dot{V}_{Cd} \\ \dot{V}_{Cq} \\ \dot{V}_{Co} \end{bmatrix} = \begin{bmatrix} 0 & w & 0 & \frac{(3D-1)}{2L} & \frac{\sqrt{3}(D-1)}{2L} & 0 \\ -w & 0 & 0 & -\frac{\sqrt{3}(D-1)}{2L} & \frac{(3D-1)}{2L} & 0 \\ 0 & 0 & 0 & 0 & 0 & \frac{1}{L} \\ -\frac{(3D-1)}{2C} & \frac{\sqrt{3}(D-1)}{2C} & 0 & 0 & w & 0 \\ \frac{\sqrt{3}(D-1)}{2C} & -\frac{(3D-1)}{2C} & 0 & -w & 0 & 0 \\ 0 & 0 & -\frac{1}{C} & 0 & 0 & 0 \end{bmatrix} \begin{bmatrix} i_{Ld} \\ i_{Lq} \\ i_{Lo} \\ V_{Cd} \\ V_{Cq} \\ V_{Co} \end{bmatrix} + \quad (5)$$

$$\begin{bmatrix} -\frac{(D-1)}{2L} & -\frac{\sqrt{3}(D-1)}{2L} & 0 & 0 & 0 & 0 & \frac{3V_{cd} - V_{gd} + \sqrt{3}V_{cq} - \sqrt{3}V_{iq}}{2L} \\ \frac{\sqrt{3}(D-1)}{2L} & -\frac{(D-1)}{2L} & 0 & 0 & 0 & 0 & \frac{3V_{cq} - V_{gq} + \sqrt{3}V_{cd} - \sqrt{3}V_{id}}{2L} \\ 0 & 0 & \frac{(D-1)}{L} & 0 & 0 & 0 & \frac{V_{go}}{L} \\ 0 & 0 & 0 & \frac{(D-1)}{2C} & -\frac{\sqrt{3}(D-1)}{2C} & 0 & -\frac{3I_{Ld} - I_{cd} + \sqrt{3}I_{Lq} - \sqrt{3}V_{oq}}{2C} \\ 0 & 0 & 0 & \frac{\sqrt{3}(D-1)}{2C} & \frac{(D-1)}{2C} & 0 & -\frac{3I_{Lq} - I_{oq} + \sqrt{3}I_{Ld} - \sqrt{3}V_{od}}{2C} \\ 0 & 0 & 0 & 0 & 0 & -\frac{(D-1)}{C} & -\frac{I_{o1}}{C} \end{bmatrix} \begin{bmatrix} V_{id} \\ V_{iq} \\ V_{io} \\ i_{od} \\ i_{oq} \\ i_{o0} \\ d \end{bmatrix}$$

The output equation is obtained as:

$$\begin{bmatrix} \hat{V}_{o1} \\ \hat{V}_{o2} \\ \hat{V}_{o3} \\ \hat{i}_a \\ \hat{i}_b \\ \hat{i}_c \end{bmatrix} = \begin{bmatrix} 0 & 0 & 0 & (1-D) & 0 & (D-1) \\ 0 & 0 & 0 & (D-1) & (1-D) & 0 \\ 0 & 0 & 0 & 0 & (D-1) & (1-D) \\ (1-D) & (D-1) & 0 & 0 & 0 & 0 \\ 0 & (1-D) & (D-1) & 0 & 0 & 0 \\ (D-1) & 0 & (1-D) & 0 & 0 & 0 \end{bmatrix} \begin{bmatrix} \hat{i}_{L_1} \\ \hat{i}_{L_2} \\ \hat{i}_{L_3} \\ \hat{V}_{C_1} \\ \hat{V}_{C_2} \\ \hat{V}_{C_3} \end{bmatrix} + \quad (6)$$

$$\begin{bmatrix} 0 & 0 & (1-D) & 0 & 0 & 0 & (V_{C_1} - V_{C_3} + V_{ca}) \\ (1-D) & 0 & 0 & 0 & 0 & 0 & (V_{C_2} - V_{C_1} + V_{ab}) \\ 0 & (1-D) & 0 & 0 & 0 & 0 & (V_{C_3} - V_{C_2} + V_{bc}) \\ 0 & 0 & 0 & 0 & (1-D) & 0 & (I_{L_2} - I_{L_1} - I_{o2}) \\ 0 & 0 & 0 & 0 & 0 & (1-D) & (I_{L_3} - I_{L_2} - I_{o3}) \\ 0 & 0 & 0 & (1-D) & 0 & 0 & (I_{L_1} - I_{L_3} - I_{o1}) \end{bmatrix} \begin{bmatrix} \hat{V}_{ab} \\ \hat{V}_{bc} \\ \hat{V}_{ca} \\ \hat{i}_{o1} \\ \hat{i}_{o2} \\ \hat{i}_{o3} \\ d \end{bmatrix}$$

Following parameters and steady state quantities are considered for deriving transfer function:

$$D = 0.33, C = 600 \mu\text{F}, C = 10 \mu\text{F}, f = 50 \text{ Hz}, I_{Ld} = 0 \text{ A}, I_{Lq} = 7.07 \text{ A}, I_{Lo} = 0 \text{ A}, V_{Cd} = 0 \text{ V}, V_{Cq} = 677.178 \text{ V}, V_{C0} = 0 \text{ V}, V_{id} = 0 \text{ V}, V_{iq} = 586.81 \text{ V}, V_{io} = 0 \text{ V}, I_{od} = 0 \text{ A}, I_{oq} = 0 \text{ A}, I_{o0} = 0 \text{ A}.$$

We can find out transfer functions with respect to desired input with help of Equations (5) and (6).

The d -axis inductor current to control the transfer function:

$$\frac{\hat{i}_{Ld}(s)}{\hat{d}(s)} = \frac{2.08 \times 10^{31} s^3 + 1.222 \times 10^{36} s^2 + 1.176 \times 10^{40} s + 6.179 \times 10^{44}}{1.594 \times 10^{26} s^4 + 1.79 \times 10^{35} s^2 - 1.945 \times 10^{20} s + 5.019 \times 10^{43}}. \quad (7)$$

The q -axis inductor current to control the transfer function:

$$\frac{\hat{i}_{Lq}(s)}{\hat{d}(s)} = \frac{1.92 \times 10^{32} s^3 + 1.295 \times 10^{35} s^2 + 1.07 \times 10^{41} s + 7.997 \times 10^{43}}{1.594 \times 10^{26} s^4 + 1.79 \times 10^{35} s^2 - 1.945 \times 10^{20} s + 5.019 \times 10^{43}}. \quad (8)$$

Similarly, d -axis capacitor voltage to control the transfer function:

$$\frac{\hat{v}_{Cd}(s)}{\hat{d}(s)} = \frac{1.303 \times 10^{32} s^3 - 1.117 \times 10^{38} s^2 + 8.13 \times 10^{40} s - 6.222 \times 10^{46}}{1.594 \times 10^{26} s^4 + 1.79 \times 10^{35} s^2 - 1.945 \times 10^{20} s + 5.019 \times 10^{43}}. \quad (9)$$

The q -axis capacitor voltage to control the transfer function:

$$\frac{\hat{v}_{Cq}(s)}{\hat{d}(s)} = \frac{-1.203 \times 10^{33} s^3 + 1.299 \times 10^{37} s^2 - 6.049 \times 10^{41} s + 7.331 \times 10^{45}}{1.594 \times 10^{26} s^4 + 1.79 \times 10^{35} s^2 - 1.945 \times 10^{20} s + 5.019 \times 10^{43}}. \quad (10)$$

3. Reliability analysis

Reliability describes the ability of any system or component to work under some specified conditions for specified time periods. The analysis has been done to check the reliability of three phase z-source converters and individual components based on specified reliability data [16]. In this section, failure rates are calculated with assumptions of constant failure rates under some pre-specified conditions.

Three phase z-source ac-ac converter has six bidirectional switches, three capacitors and three inductors. The calculation of the failure rate of each component of the converter system is given below:

3.1. Capacitor

Part failure rate $\lambda_p = \lambda_b \pi_{CV} \pi_Q \pi_E$ failures/ 10^6 h [16]

$$\lambda_b = 0.00115 \left[\left[\left(\frac{S}{0.4} \right)^5 + 1 \right] \exp \left(2.5 \frac{(T + 273)}{358} \right)^{18} \right],$$

where:

$$S = \frac{\text{Operating voltage}}{\text{Rated voltage}} = \frac{V_{DC} + \sqrt{2}V_{ACrms}}{V_{DCrated}}$$

Then $\lambda_b = 0.00037$ at $S = 0.1$ and $T = 70^\circ\text{C}$, $\pi_{CV} = 1.4C^{0.12} = 1.8455$ for $C = 10 \mu\text{F}$, $\pi_Q =$ quality factor = 10 for commercial and unknown screening level, $\pi_E =$ environmental factor = 10 for fixed ground.

For a commercial, ground fixed, paper di-electric capacitor of capacitance $C = 10 \mu\text{F}$ with $S = 0.1$ at $T = 70^\circ\text{C}$.

The failure rate becomes as:

$$\lambda_p = 0.00037 \times 1.844 \times 10 \times 10 = 0.683 \text{ failures}/10^6 \text{ h.}$$

3.2. Inductor

Part failure rate $\lambda_p = \lambda_b \pi_c \pi_Q \pi_E$ failures/ 10^6 h [16], where

$$\lambda_b = 0.000335 \left[\exp \left(\frac{(T_{HS} + 273)}{329} \right)^{15.6} \right].$$

T_{HS} is the hot spot temperature ($^\circ\text{C}$), $T_{HS} = T_A + 1.1(\Delta T)$ ($^\circ\text{C}$), ΔT is the average temperature rise above ambient.

So, $\lambda_b = 0.0023$ at 75°C for a fixed inductor, $\pi_c = 1$ for a fixed inductor, $\pi_Q =$ quality factor = 3.0, 1.0, for lower quality, $\pi_E =$ environmental factor = 6.0 for grounded and fixed devices.

For a fixed inductor the failure rate:

$$\lambda_p = 0.0023 \times 1.0 \times 3.0 \times 6.0 = 0.0414 \text{ failures}/10^6 \text{ h.}$$

3.3. High frequency switches

Part failure rate $\lambda_p = \lambda_b \pi_T \pi_Q \pi_E$ failures/ 10^6 h [16] where $\lambda_b =$ base failure rate = 0.0083 for IGBT.

$$\pi_T = \exp \left[-2489 \left(\frac{1}{T_j + 273} - \frac{1}{298} \right) \right].$$

Temperature factor $\pi_T = 3.0$ for $T_j = 75^\circ\text{C}$, $\pi_Q =$ quality factor = 5.5 for lower or commercial quality, $\pi_E =$ environmental factor = 2.0 for grounded and fixed devices, $\lambda_p = 0.0083 \times 3.0 \times 5.5 \times 2.0 = 0.2739$ failures/ 10^6 h.

Therefore, failure rate of the total system (considering the total number of components used) is:

$$\lambda_{\text{SYSTEM}} = 6 \times \lambda_{\text{SWITCH}} + 3 \times \lambda_{\text{CAPACITOR}} + 3 \times \lambda_{\text{INDUCTOR}} = 3.1866 \text{ failures}/10^6 \text{ h.}$$

Mean time to failure is then calculated as:

$$MTTF = \frac{1}{\lambda_{\text{SYSTEM}}} \text{hours} = 3816600 \text{ hours} .$$

4. Results and discussion

Verification of modeling is carried out using hardware-in-the-loop (HIL) and offline simulation of a closed loop converter system using a real-time simulator and MATLAB/Simulink respectively. The z-source network parameters are selected as $L_1 = L_2 = L_3 = 0.6$ mH, and $C_1 = C_2 = C_3 = 10$ μ F. Switching frequency is chosen as 10 kHz and the proposed model computed in a real-time simulator with a fixed-time step of 10 μ s. The PID tuning parameters are selected with the help of the SISO tool in MATLAB such as $K_p = 1.8$, $K_I = 5$ and $K_d = 0.05$. OPAL-RT simulator comprises the distinctive characteristic of combining conventional phasor-type solver with ephasor sim with calculated real-time step solver. Real-time simulation results provide a bridging gap between the incorporating software and hardware. A bi-directional switch is realized connecting two IGBTs in anti-parallel. A PID controller is employed for the generation of variable PWM signals for the switches of a converter. A controller is designed on the basis of small signal analysis. The controller operates in feed-forward mode through sensing the voltage across the impedance network capacitor and modulated the PWM duty of the converter. During step load changes, the closed loop system with a PID controller is employed to and compensated the PWM duty of the converter. The output voltage has small variation for a wide range of step load changes and no effect on the circuit performance. The controller provides constant and smooth output voltage during load variations.

The simulation result is shown in Table 1 at different input voltage. The input line voltage is varied from 370 V to 610 V and output voltage is observed almost constant around 400 V. The output voltage has small variation for a wide range of input voltage. A closed loop control system provides steady state output voltage during voltage sag and surge. Input line voltage is suddenly varied from 370 V to 260 V from 0.7 s to 0.8 s during voltage sag and the output voltage waveform is captured. The input and output voltage and corresponding input current waveforms are shown in Fig. 4. During surge, input voltage is varied suddenly from 370 V to 480 V from 0.7 s to 0.8 s and waveforms are recorded as shown in Fig. 5.

Table 1. Three phase z-source AC-AC converter at different input voltage condition

Input Voltage (rms), V_{in}	Output Phase Voltage (rms), V_{out}	Gain, G
370 V	391.2 V	1.05
390 V	393.5 V	1.00
420 V	396.4 V	0.943
490 V	398 V	0.812
520 V	405 V	0.778
580 V	410.5 V	0.707
610 V	414 V	0.678

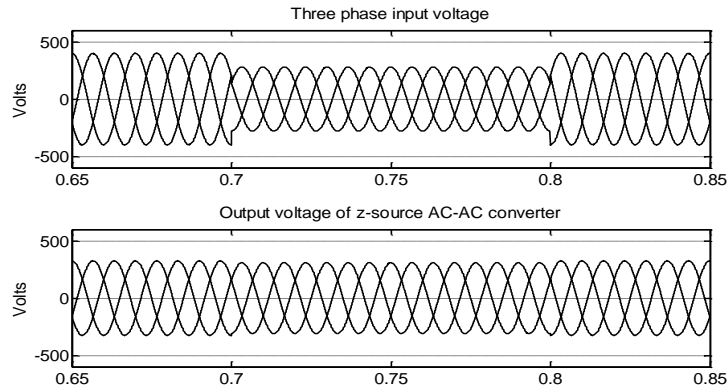


Fig. 4. During voltage sags condition the following waveform: (a) input voltage; (b) output voltage

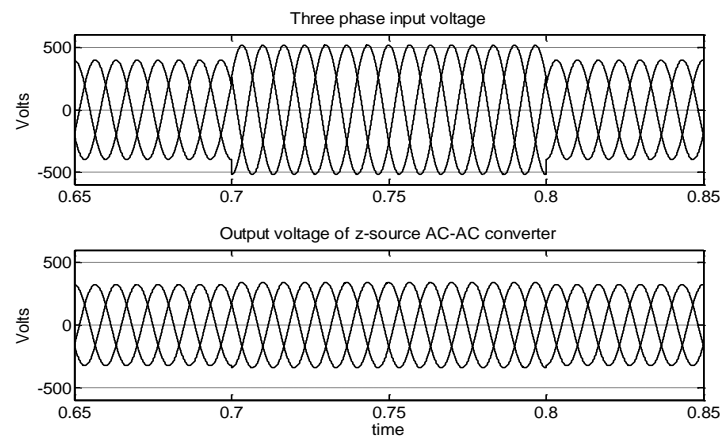


Fig. 5. During voltage surge condition following waveforms (a) input voltage (b) output voltage

Real-time HIL simulation waveforms are captured in DSO at fixed-time step $10 \mu\text{s}$ during supply voltage variation. Fig. 6 and Fig. 7 have shown the nature of output voltage during voltage sag and surge respectively. For a wide variation of input voltage, the output voltage is approximately constant around 400 V rms during both voltage sag and surge conditions. During the sudden change in input voltage, the output voltage and settling time of the system is effectively less due to an appropriate PID controller coefficient selection. The controller provides constant and smooth output voltage during supply voltage variations.

5. Conclusions

This paper presents modeling and reliability analysis of a three phase z-source ac-ac converter. Modeling of the three phase z-source converter is done using the small signal analysis in a state space averaging technique.

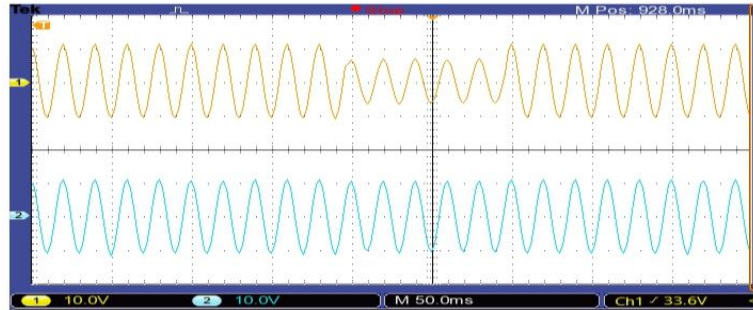


Fig. 6. HIL simulation waveforms (in reduced scale) during voltage sags condition: channel 1-input voltage; channel 2-output voltage of z-source ac-ac converter

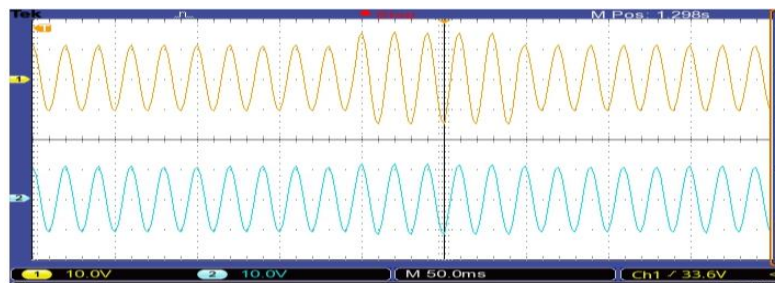


Fig. 7. HIL simulation waveforms (in reduced scale) during voltage surge condition: channel 1-input voltage; channel 2-output voltage of z-source ac-ac converter

Three phase z-source ac-ac converter based system acts as a novel solid state transformer with controllable transformation ratio. A control transfer function is derived with the help of small signal analysis. The closed loop control system with a PID controller provided steady state output voltage during voltage sag and surge. The output voltage of the converter is almost unaffected and remains constant during supply voltage variation. The real-time HIL and offline simulation results verify the theoretical concept and performance of the z-source converter system. Z-source ac-ac converter has constant output voltage during voltage fluctuations. The real-time HIL testing reduces development and design cost before implementation in real field. The reliability analysis of the z-source converter system and individual components are calculated. The failure rate and mean time to failures are calculated for a three phase converter system and individual component. The reliability-based design increases efficiency, accuracy and robustness of the system for wide applications.

References

- [1] Razzaghi R., Mitjans M., Rachidi F. et al., *An automated FPGA real-time simulator for power electronics and power systems electromagnetic transient applications*, Electric Power System Research, vol. 141, pp. 147-156 (2016).
- [2] Higashikawa K., Urasaki S., Inoue M. et al., *Hardware-in-the-loop simulation of superconducting devices for DC electric railway systems based on a real-time digital simulator*, IEEE Trans. on Applied Superconductivity, vol. 26, no. 4 (2016).

- [3] Prasad H., Maity T., *Real-time simulation for performance evaluation of bidirectional quasi z-source inverter based medium voltage drives*, COMPEL-The International Journal for Computation and Mathematics in Electrical and Electronic Engineering, vol. 35, no. 3, pp. 1123-1135 (2016).
- [4] Tavana N.R., Dinavahi V., *A general framework for FPGA-based real-time emulation of electrical machines for HIL applications*, IEEE Trans. on Ind. Electronics, vol. 62, no. 4, pp. 2041-2053 (2015).
- [5] Prasad H., Maity T., *Real-time performance analysis of modified z-source inverter-fed induction motor drives using xilinx system generator*, EPE Journal, vol. 26, no. 4, pp. 142-152 (2016).
- [6] Peng F.Z., *Z-Source Inverter*, IEEE Trans. on Ind. Appl., vol. 39, no. 2, pp. 504-510 (2003).
- [7] Fang X.P., Qianand Z.M., Peng F.Z., *Single-Phase Z-Source PWM AC-AC Converters*, IEEE Power Electronics Letters, vol. 3, no. 4, pp. 121-124 (2005).
- [8] Prasad H., Maity T., Singh V.K., *A Simple Transformerless Buck-Boost Switching Voltage Regulator*, Asian Power Electronics Journal, vol. 8, no. 2, pp. 57-61 (2014).
- [9] Prasad H., Maity T., Singh V.K., *Transformer less Voltage Regulator*, IEEE International Conf. on Green Computing, Communication and Electrical Eng., pp. 1-5 (2014).
- [10] Fang X., *Three Phase Z-Source AC-AC converter*, IEEE International Power Electronics and Motion Control Conference, pp. 621-624 (2006).
- [12] Zhang F., Fang X., Peng F.Z., Qian Z., *A New Three Phase AC-AC Z-Source Converter*, IEEE Applied Power Electronics Conference and Exposition, pp. 123-126 (2006).
- [13] Sonar S., Maity T., Minu M., *Single phase transformerless wide range ac boost voltage regulator based on z-source network*, International Journal of Electrical Power & Energy System, vol. 47, pp. 193-197 (2013).
- [14] Liu J., Hu J., Xu L., *Dynamic Modeling and Analysis of z-Source converter – Derivation of AC Small Signal Model and Deigns-Oriented Analysis*, IEEE Trans. on Power Electronics, vol. 22, no. 5, pp. 1786-1796 (2007).
- [15] Galigekere N.V.P., Kazimierczuk M.K., *Small-Signal Modeling of Open-loop PWM Z-Source Converter by Circuit-Averaging Technique*, IEEE Trans. on Power Electronics, vol. 28, no. 3, pp. 1286-1296 (2013).
- [16] Gajanayake C.J., Vilathgamuwa D.M., Loh P.C., *Small-Signal and Signal-Flow-Graph Modeling of Switched Z-Source Impedance Network*, IEEE Power Electronics Letters, vol. 3, no. 3, pp. 111-116 (2005).
- [17] Loh P.C., Vilathgamuwa D.M., Gajanayake C.J. et. al., *Transient Modeling and Analysis of Pulse-Width Modulated Z-Source Inverter*, IEEE Trans. on Power Electronics, vol. 22, no. 2, pp. 2782-2789 (2007).
- [18] Prasad H., Maity T., *Design of a Stable and Efficient Z-Source AC-AC Converter using Small Signal Analysis*, IEEE Power, Communication and Information Technology Conf., pp. 190-194, (2015).
- [19] Rim C.T., Hu D.Y., Cho G.H., *Transformers as Equivalent Circuits for Switches: General Proofs and D-Q Transformation-Based Analysis*, IEEE Transformations on Industry Applications, vol. 26, no. 4, pp. 777-785 (1990).
- [20] Masrur M.A., *Studies on the Effect of Filtering, Digitization, and Computation Algorithm on the ABC-DQ Current Transformation in PWM Inverter Drive System*, IEEE Trans. on Vehicular Technology, vol. 43, no. 2, pp. 356-365 (1995).
- [21] Galigekere V.P., Kazimierczuk M.K., *Analysis of PWM z-source DC-DC converter in CCM for steady state*, IEEE Trans. Circuits and Systems, Part I, regular papers, vol. 59, no. 3, pp. 854-863 (2012).
- [22] Chan N., *A Generalized Reliability Function for Systems of Parallel Components*, IEEE Trans. on Reliability, vol. 17, no. 2, pp. 199-201 (1968).
- [23] Todri A., Marek-Sadowska M., *Reliability Analysis and Optimization of Power-Gated ICs*, IEEE Trans. on very Large Scale Integration (VLSI) Systems, vol. 19, no. 3, pp. 457-468 (2011).
- [24] Alam M.K., Khan M.H., *Reliability Analysis and Performance Degradation of a Boost Converter*, IEEE Trans. on Industry Applications, vol. 50, no. 6, pp. 3986-3994 (2014).
- [25] Military Handbook, *Reliability Prediction of Electronic Equipment*, Washington, DC, USA (1991).